The Role of Unsteadiness within a Central Jet on the Structure of a Combined Central and Co-annular Jet Flow

N.L. Smith[1] and G.J. Nathan[2]

[1]Department of Chemical Engineering

[2]Department of Mechanical Engineering
Adelaide University, South Australia, 5005 AUSTRALIA

Abstract

Qualitative and quantitative assessments of the effect of the unsteadiness in a central precessing jet (PJ) on a co-annular jet were made using experimental methods. The central jets were an unsteady PJ, a simple axial jet, a simple jet directed at 45° to the nozzle axis and a conical jet directed at 45° to the nozzle axis. The central jets were compared on the basis of similar axial momentum. The simple directed jet corresponds to case in which the PJ flow has a precession frequency of zero and the conical jet corresponds to the case with a precession frequency of infinity. Experimental investigations of the near-nozzle region were performed in water using a two-colour planar laser induced fluorescence visualisation technique.

The visualisations showed that, like the PJ flow, both the directed and the conical jets increased the initial spread of the combined flow. Nevertheless the PJ flow is fundamentally different from the steady analogues. The PJ flow was the only flow to increase the scale of the large-scale, visually coherent, motions in the combined flow. This observation was quantified by measurements of jet half-width. The central PJ flow increased the annular jet half width by 66%, while the steady jets reduced it by 7% - 32 %.

Introduction

Precessing jets (PJ) are a class of unsteady flow that have found application in combustion [7,10]. The emerging jet from a PJ nozzle is, at any instant, directed at a large angle to the nozzle axis. The azimuthal direction of the emerging jet oscillates with time. Both the angle of the emerging jet and the dimensionless frequency of its oscillation, described by a Strouhal number, have been found to significantly influence the size of large-scale turbulent structures in the jet in an unconfined environment [9,5]. However the role of these parameters in a PJ flow interacting with a co-annular co-flowing jet has yet to be investigated.

Annular jets are often used in pulverised fuel (PF) burners to convey the particulate phase. In a rotary kiln burner additional nozzles are located centrally within the annular PF stream, either for ignition or for influencing the mixing rates of the PF with the co-flowing combustion air. Recent pilot-scale trials have shown that the use of a PJ nozzle located centrally within the annular PF stream can beneficially influence the flame [3]. Typically the ignition distance can be reduced by a factor of 5, bringing the heat-release closer to the nozzle, and reduced NOx emissions are also measured.

The mechanisms by which unsteady jets may influence both a co-annular flow and a flame are still poorly understood. Visualisations of a two-phase, non-reacting annular jet combined with a central PJ flow of air, have shown that the trajectories of the particles are deflected significantly by the central unsteady PJ flow in the region, $x/D \leq 3$ [11], where x is the distance downstream from the nozzle exit plane and D is the PJ nozzle diameter. This initial deflection of the particles and the enhancement of large-scale turbulent structures by PJ flows are deduced to contribute to "clustering" of particles. Within a flame, clustering is deduced to contribute to fuel-rich combustion

and soot formation [3,11]. The relative momentum of the PJ, annular and surrounding co-flows control the extent of clustering.

Clearly, both the unsteadiness of the PJ and the fact that it is directed at a large angle to the nozzle influence these co-annular two-phase flows and flames. To explore the relative significance of these two phenomena and to provide more insight into the influence of a central PJ flow on a co-annular stream, a flow visualisation study was undertaken. The study compares several analogous flows in which the central "bluff body" in an annular jet can be replaced by other inter-changeable central nozzles.

Apparatus and Procedures

The nozzles are illustrated in Fig.1. Fig.1a shows the annular channel with a bluff body on the axis. The interchangeable central jet nozzles are illustrated in Figs. 1b - 1e. Fig. 1b shows a PJ nozzle, D =19 mm. Each of the "steady analogues" of the PJ (Figure 1c – 1e) were designed to have a nozzle cross-sectional exit area equal to the nominal value of the jet emerging from the PJ nozzle. In this way, the combined central jet – annular flows can be characterised and compared on the basis of similar axial momentum and velocity ratios, by using equal flow-rates. The nominal area of the emerging PJ flow is deduced to be one third of the area between the nozzle wall and the centre-body (shown in Figure 1b) [2]. The nozzles shown in Figure 1c – 1e are a "conically diverging" annular jet, a steady axial jet, and a steady jet directed at a 45° to the nozzle axis, respectively. The jet exit angle of 45° matches the exit angle of the instantaneous PJ to the nozzle axis [8]. The steady 45° directed jet corresponds to a precession frequency of zero and the conical jet corresponds to a precession frequency of infinity. Both jets eliminate the large-scale unsteadiness associated with the PJ.

In all visualisations the laser sheet was aligned to pass through the nozzle axis (Figure 2). The support legs of the central cone of the conical nozzle are found to influence the flow. To observe this effect the light sheet is aligned so that the left and right sides of the image correspond to the locations of maximum and minimum interference respectively, as shown in Figure 1(c).

The experiments were conducted in water in a perspex tank using a Laser Induced Fluorescence (LIF) technique (Figure 2) [4]. The central and annular jets contained different dyes at concentrations of 0.1g/l, Rhodamine B, which fluoresces red, or Fluorescein, which fluoresces yellow/green. The ambient fluid was unmarked. A 3mm thick light sheet was created from a 5W Ar-ion laser and aligned with the nozzle centre-line. Images were recorded on video-tape.

The annular flow was set at 592 l/hr and the central "mixing" flows were all 250 l/hr, corresponding to an exit velocity of 1.95 ms^{-1}. These conditions ensured the nominal axial momentum ratio of central "mixing" to annular flow was $G_{MIX}/G_1 = 2.56$ in each case, corresponding to that used in combustion experiments [12]. Here G is defined as the momentum flux (N) of a jet in its exit direction, equal to the product of its mass flow rate and area average velocity. The Reynolds number at the PJ inlet was 23,300, which is sufficient to ensure consistent precession [1].
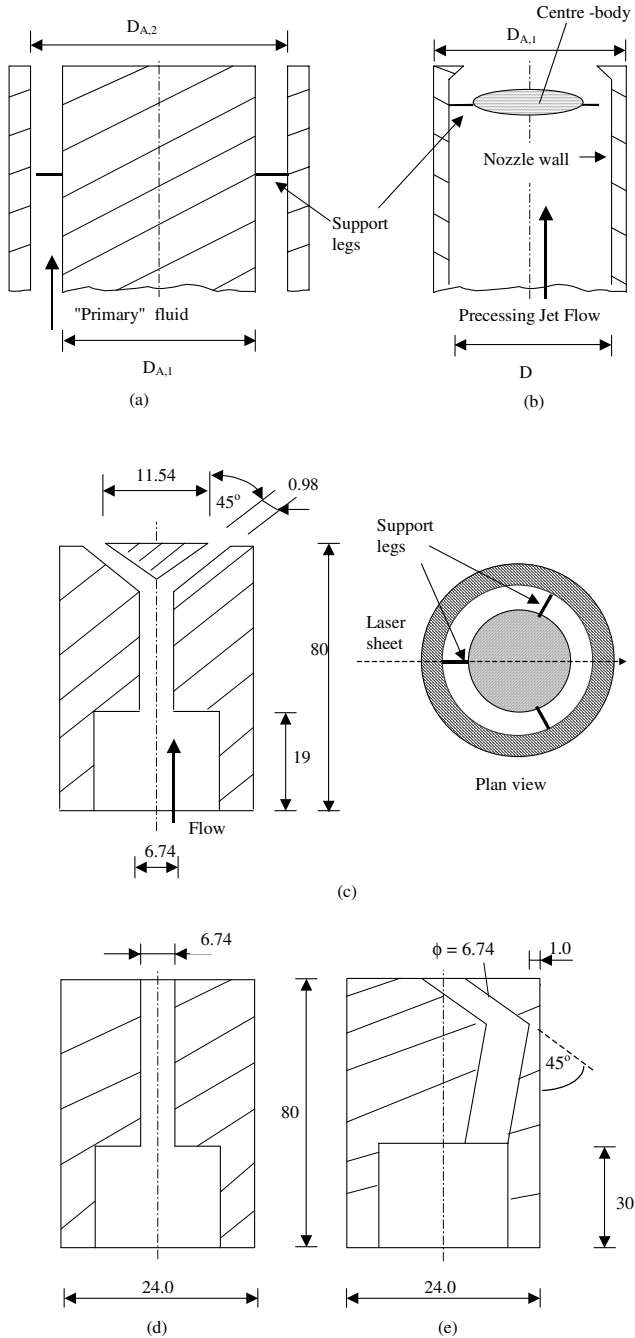
Figure 1. Nozzles used in the water LIF experiments.

(a) Annular, $D_{A,1}$ = 24.0 mm, $D_{A,2}$ = 32.5 mm.
(b) PJ nozzle, two nozzles with D = 19 mm, $D_{A,1}$ = 24 mm
(c) Conically diverging jet
(d) Simple axial steady jet d = 6.74 mm (not deflected at exit)
(e) 45° angled jet, d = 6.74

Experiments were also performed using a single colour LIF technique in which only the annular stream was marked. This allows the half width of the co-annular flow to be determined for each of the combined flows. The limitations of spatial resolution and signal-to-noise ratio of the present technique mean that it is unsuitable for detailed statistical measurements. However the determination of half-width does not require high signal-to-noise ratio nor good spatial resolution, since it is based on mean data. For the present analysis it is assumed that beam divergence causes only axial variation in beam intensity, that signal attenuation is negligible and that there is no variation in the

intensity of the laser beam [4]. Hence normalisation is only required in the local radial direction. The errors associated with the above assumptions are estimated to be within ± 10 %, which is comparable with the accuracy of the rest of the system and is sufficient to quantify large differences in flow features.
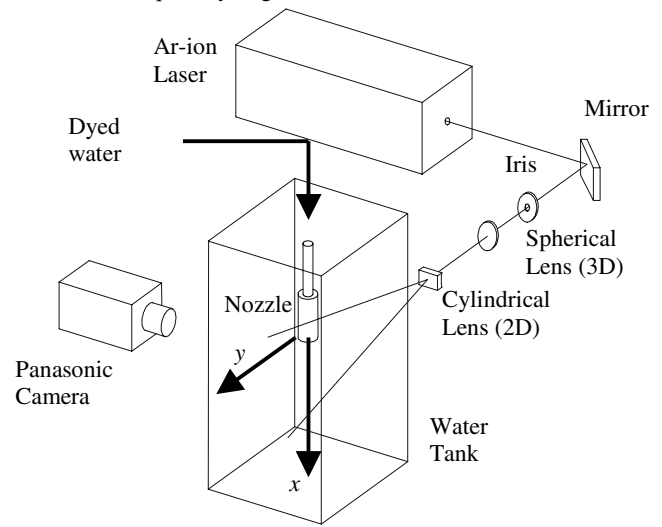

Figure 2. A schematic diagram of the experimental arrangement used for planar laser-induced fluorescence (PLIF) experiments in the water tank facility for flow visualisation [4].

Video images were converted to 8 bit greyscale 640x480 pixel images. Each pixel images a 0.4 x 0.4 mm section of the jet. Using commercial software "Transform", 40 digital images are summed and averaged to provide a mean flow field. Since the flow is directed from the top of the image, each row of the mean digital image represents positions of equal $x/D_{A,2}$. A background concentration correction is performed and each pixel in the corrected average image is then divided by the maximum value in its own row. The final image is thus a normalised mean image in which the concentration of marked fluid in each pixel, $\overline{\xi}$ is expressed as a fraction of the maximum value at the corresponding axial position, $x/D_{A,2}$. This equates to a normalised mixture fraction, $\overline{\xi} / \overline{\xi}_{max}$.

Results of Flow Visualisations

Figure 3 presents instantaneous images of a slice of the flow aligned with the geometric centre of the combined nozzles. The use of two colours allows the two flows to be distinguished. (Note that two colours were used in all cases except the conical jet, where only the annular flow was marked.) It is apparent that the PJ, conical jet, and directed jet all increase the initial spreading rate of the combined jets relative to the central axial jet. However each of the flows are quite different. Note that the combined mean flows from the conical and directed jets are not axially symmetric.

In the near field, the directed jet "punches through" the co-annular jet rather than merging with it so that the two jets only merge to a small extent. In contrast, the PJ merges with the annular flow so that the combined flow behaves more like a single jet, which is consistent with the trend found for a configuration in which the PJ was the outer flow and the central jet was axial [6]. The conical jet causes the combined jet to spread rapidly in the near field. Interestingly there is no evidence of increased central recirculation that might be anticipated for a "bluff body" type configuration. That the conical jet increases fine-scale, rather than large-scale, mixing is consistent with the much narrower annular gap required to ensure similar momentum to that of the other central jets.
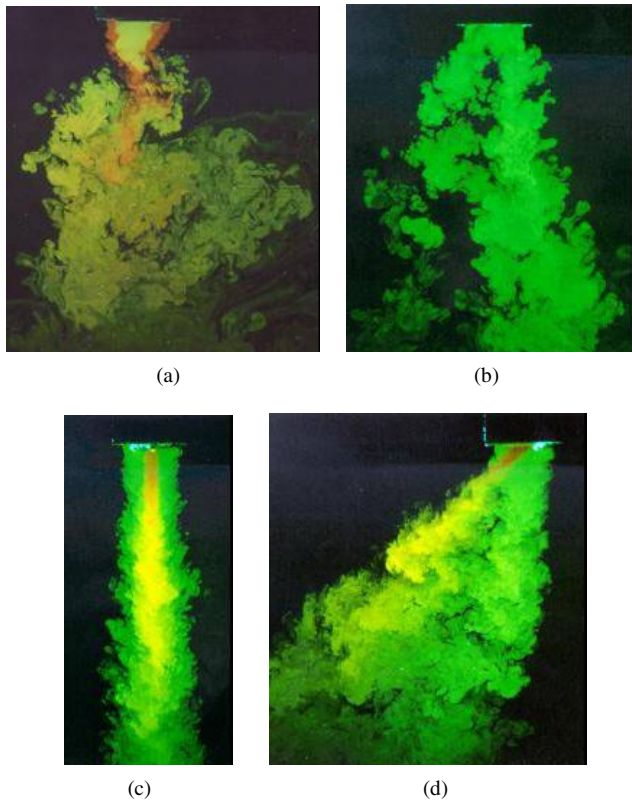
(a) (b)

(c) (d)

Figure 3 Typical images of combined central and annular flows. (a) PJ, (b) conical jet, (c) simple axial jet, (d) 45° directed jet. (Fig 3b shows a case when only the annular stream was marked.)

Importantly, the visualisations provide strong evidence that only the unsteady PJ flow causes a significant increase in the scale of mixing of the combined flow. All other flows act to promote fine-scale mixing. Likewise, only the PJ flow produces motions which are visually coherent across the almost entire width of the of the combined flow. It is clear that the unsteadiness of the PJ flow is significant and dramatically alters the structure of the annular flow relative to the steady-flow analogues.

Jet Half Angles and Half Widths

The contours for which the concentration is half of the local maximum have been calculated in the region $0 \le x / D_{A,2} \le 3$.

Figure 4 shows the locally normalised mean concentration map of the annular jet alone. The red pseudo-colour is used for values of $\overline{\xi} / \overline{\xi}_{\max} > 0.5$, blue for $\overline{\xi} / \overline{\xi}_{\max} < 0.5$ and white for the transition. The locally normalised 0.5 concentration contour is also shown. The initial jet half angle, $\theta_{1/2}$, is calculated by drawing a straight line along the roots of the 0.5 concentration contour in the initial region of the jet (Fig. 4). The jet half width, $r_{1/2}$, can be calculated from $\theta_{1/2}$. However, here the 50% contours on either side of the jet are used to determine $r_{1/2}$ because it is the most appropriate method for the angled steady jets as outlined below. The apparent reduction in the width of the annular jet at the downstream end of the image is caused by reduced signal-to-noise in this region, associated with high background dye concentration and reduced jet fluid concentration. The effect is insignificant in the near nozzle region.

Figure 5 shows locally normalised mean concentration plots for combined flows with $G_{MIX}/G_1 = 2.56$. Fig. 5a demonstrates the dramatic influence of the PJ on the annular flow. In the initial region $0 \le x / D_{A,2} \le 2$, the combined flow spreads rapidly at a mean half angle of 29°. The rate of spread then reduces, so that

over the larger region, $0 \le x / D_{A,2} \le 3$, the mean half angle is 23°, still a dramatic increase over that of the annular jet alone (5.6°). The jet half width, calculated from 50% contours on both sides of the jet at $x/D_{A,2} = 3$, is 1.23$D_{A,2}$.
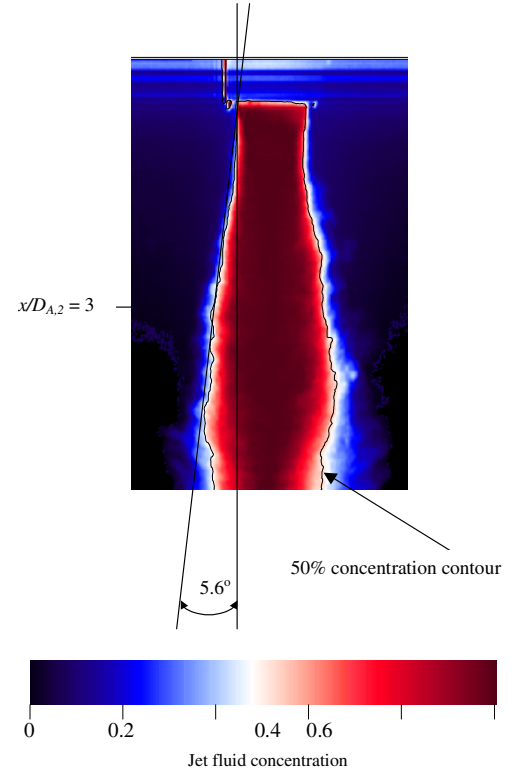

Figure 4 Normalised mean fluid concentration map of annular jet showing the jet half angle, $\theta_{1/2}$, and the axial location at which the half width $r_{1/2}$, is measured.

In contrast to the PJ flow, the half angle of the co-axial jet (Fig. 5b) is consistent throughout the region, $0 \le x / D_{A,2} \le 3$ and, at 3.4°, is less than that of the annular jet alone, presumably because the central jet entrains the annular jet into it. The half width of the co-axial jet at $x/D_{A,2} = 3$, is 0.50$D_{A,2}$.

The "conically diverging" jet interacts with the annular jet to produce a conical fan (Fig. 5c). The present images suggest that the most accurate representation of the scale of the dominant structures can be obtained by considering each side of the fan separately. The right fan of the jet is taken to be representative of the entire jet, as discussed earlier. Since the right fan of the jet is not symmetrical about the nozzle axis, the total angle between straight lines drawn along the 50 % contours on each side of the fan is measured and halved to give a half angle, $\theta_{1/2}$, of 8.6°. Using the same straight lines at $x/D_{A,2} = 3$, $r_{1/2} = 0.52D_{A,2}$.

Fig. 5d shows that, when combined with the annular jet, the 45° directed jet produces a non-symmetric jet. The bulk of the annular fluid maintains a generally axial trajectory, whilst only a fraction of it is entrained into the directed jet. A region of low concentration annular fluid can be found between the two jets. The large-scale structures in the near-field of this flow are thus best characterised separately for each of the two sections of the jet. The right side of the jet is dominant and has $\theta_{1/2} = 8.3°$ and $r_{1/2} = 0.69D_{A,2}$ at $x/D_{A,2} = 3$.

In contrast, to the conically diverging and 45° directed jets, the combined PJ - annular jet is three dimensional and symmetric so the measured half-width genuinely represents the scale of the dominant structures, which are substantially greater than all other mixing nozzles tested. In the PJ flow investigated here the

precession frequency is ~ 4 Hz so that variations in the direction of the emerging jet can be observed in consecutive video frames. However true precession only occurs within the region close to the nozzle $x/D < 1$, beyond which it undergoes a transition to a jet flow whose with characteristic large scale motions span the entire width of the merged flow. This type of flow occurs over a wide range of Strouhal numbers [5]. The data presented in Table 1 demonstrates that the PJ flow enhances large-scale structure in the annular flow relative to all other nozzles.
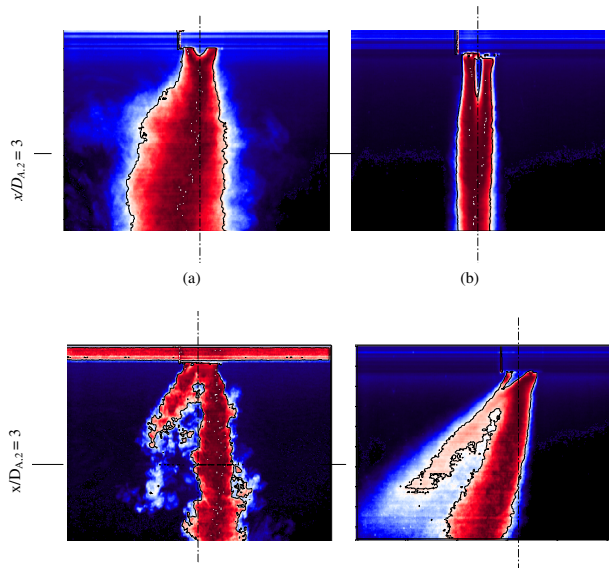

Figure 5 Normalised mean concentration of annular fluid in the 4 types of combined co–annular flow, with G_{MIX}/G_1 = 2.56.
(a) PJ, (b) simple co-axial jet, (c) conically diverging jet, (d) simple 45° directed jet

Jet	$r_{1/2}/D_{A,2}$ (at $x/D_{A,2}$ =3)
PJ	1.23
Co-axial	0.50
Conically diverging	0.52
45° directed	0.69
Annular*	0.74

Table 1 Half widths of combined jets with G_{MIX}/G_1 = 2.56
*The annular jet is included for comparison

Conclusions

The present study has compared the influence of a range of different types of central jet nozzle on the near-field structure of a co-annular flow. Both the visualisations and the measurements of half-width support the conclusion that the influence of the unsteady precessing jet on the annular flow is dramatically different from that of the analogous steady jets. The unsteady central PJ acts to increase the dominant scale of mixing, while all other flows act to promote fine-scale mixing between the two flows. The central PJ flow increases the annular jet half width, $r_{1/2}/D_{A,2}$ from 0.79 to 1.23 at $x/D_{A,2}$=3, whereas all of the steady jets act to reduce the annular jet half width.

The visualisations show that it is the unsteadiness of the PJ flow, and not simply the angle at which the emerging jet leaves the nozzle, which is an essential element of the flow. The steady jet, directed at an angle comparable to the instantaneous direction of the emerging PJ flow, "punches through" the outer annular flow.

In contrast the PJ combines with the annular jet. Likewise the "conically diverging" jet combines with the annular jet, but promotes fine-scale rather than large-scale mixing and does not promote visually coherent motions that span the entire width of the combined flow. The unsteadiness of the PJ flow has implications for the development of models, as well as practical burner devices.

References

[1] Nathan, G.J., Nobes, D.S. Mi J., Schneider, G.M., Newbold, G.J.R., Alwahabi, Z.T., Luxton., R.E. and King, K.D. Exploring the Relationship Between Mixing, Radiation, and NO$_x$ Emissions from Natural Gas Flames. *Combustion and Emissions Control III'*, 1997, 49-69.

[2] Nathan, G.J., Smart, J.P. and Jenkins, B.G. Criterion for Modelling Gyrotherm Burners. *FCT Ltd.Internal Report*.

[3] Nathan, G.J., Smith, N.L., Mullinger, P.J. and Smart, J.P. (2000) Performance Characteristics of, and an Aerodynamic Scaling Parameter for, a Practical PF Burner Design Employing Jet Excitation to Promote Particle Clustering. *5th Intl. Conf. on Industrial Furnaces and Boilers (INFUB)*, 2000.

[4] Newbold, G.J.R. *Mixing and Combustion in Precessing Jet Flows*. PhD. Thesis, Adelaide University, 1997.

[5] Nobes, D.S *The Generation of Large-scale Structures by Jet Precession*. PhD. Thesis, Adelaide University, 1998.

[6] Parham, J.J., Nathan, G.J. and Alwahabi, Z.T. The Influence of a Co-flow on the Instantaneous Structure of a Confined Precessing Jet Flow. *Album of Visualization*, The Visualization society of Japan, 2000.

[7] Parham, J.J., Nathan, G.J., Smart, J.P., Hill, S.J. and Jenkins, B.G. The Relationship Between Heat Flux and NOx Emission in Gas Fired Rotary Kilns. *J. Inst. Energy* **73**, 2000, 25-34.

[8] Schneider, G.M. *Structure and Turbulence Characteristics in a Precessing Jet Flow*. PhD Thesis, Adelaide University, 1996.

[9] Schneider, G.M., Froud, D., Syred, N., Nathan, G. J., and Luxton, R.E. (1997) Velocity Measurements in a Precessing Jet Flow using a Three Dimensional LDA System.. *Experiments in Fluids*, **23**, 89 –98.

[10] Smart, J.P., Nathan G.J., Smith, N.L., Newbold, G.J.R., Nobes, D.S. and Morgan, D.J. (1999) Further Developments in Precessing Jet Burner Technology, *5th Intl. Conf. on Tech. and Combn. for a Clean Environment*.

[11] Smith, N.L. *The Influence of the Spectrum of Jet Turbulence on the Stability, NO$_x$ Emissions and Heat Release Profile of Pulverised Coal Flames*. PhD. Thesis, Adelaide University, 2000.

[12] Smith, N.L., Megalos, N.P., Nathan, G.J., Zhang, D.K., and Smart, J.P. The Role of Fuel Rich Clusters in Flame Stabilisation and NO$_x$ Emission Reduction with Precessing Jet PF Flames. *27th Symp. Combn*, 1998, 2, 3173 - 3179.

Nomenclature

D	Precessing jet nozzle diameter
$D_{A,1}$	Annular channel inside diameter
$D_{A,2}$	Annular channel inside diameter
G_{MIX}	Momentum flux of central "mixing" jet
G_1	Momentum flux of annular jet
$r_{1/2}$	Jet half width
PJ	Precessing Jet
x	Axial distance downstream from nozzle exit plane
$\overline{\xi}$	Concentration of marked fluid in mean image
$\overline{\xi}_{max}$	Maximum concentration at any given x
$\theta_{1/2}$	Jet half angle